EVALUATION OF THE KURTOSIS ALGORITHM IN DETECTING RADIO FREQUENCY INTERFERENCE FROM MULTIPLE SOURCES

Sidharth Misra, Roger De Roo and Christopher Ruf
Department of Atmospheric, Oceanic and Space Sciences
University of Michigan
Ann Arbor, MI 48109-2143

***Abstract* – A few of the issues faced by the kurtosis detection algorithm on recent field campaigns is discussed here. The performance of the kurtosis algorithm in detecting multiple-source Radio Frequency Interference (RFI) is characterized. A new RFI statistical model is presented in the paper to take into account the behavior of RFI sources under a large foot-print. Results indicate the behavior of the kurtosis ratio under central-limit conditions due to large number of RFI sources.**

***Index Terms* – Microwave radiometer, radio frequency interference, kurtosis**

I. INTRODUCTION

Radio-Frequency Interference (RFI) is a serious detriment to science measurements made by passive microwave remote-sensing instruments. Brightness temperature (Tb) measurements made in the L-, C- and X-band have been found to contain man-made interference signals in them [8,9,15-18]. If left unmitigated, the resulting Tb values can cause erroneous retrieval of science estimates. As a result, active steps are being taken to mitigate RFI in future missions.

The Soil Moisture Active/Passive (SMAP) mission is one of the high priority missions identified in the recent NRC Earth Decadal Survey [19]. It will produce global maps of soil-moisture estimates from active and passive observations at L-band. The SMAP mission is implementing the kurtosis detection algorithm as its primary RFI mitigation option. The kurtosis detection algorithm has been successfully tested and proven in many field-campaigns [1, 6-9]. These campaigns demonstrate the capability of the kurtosis detector in detecting RFI around the noise-level of the radiometer.

This paper discusses the performance of the kurtosis detection algorithm when simultaneously observing many RFI-sources. Considering the relatively high altitude of satellite missions compared to airborne missions, it is likely that many sources exist in the large foot-print of the radiometer antenna. Since the kurtosis detector works on the principle of observing a Gaussian distributed signal, the effects of central-limit like conditions are evaluated in the paper. The next section presents a brief description of the kurtosis detection algorithm and blind-spots associated with the detection algorithm. Section III introduces a new RFI model to take into account multiple sources and the results are presented in section IV. The paper is summarized in section V.

II. KURTOSIS ALGORITHM AND ISSUES

The kurtosis RFI detector identifies RFI in the amplitude domain or statistical domain by measuring the higher-order moments of the incoming pre-detected voltage signal from a radiometer [1]. The detection algorithm is independent of the incoming power, hence Tb variations, and is an effective tool for detecting low-level RFI compared to other detection algorithms [2].

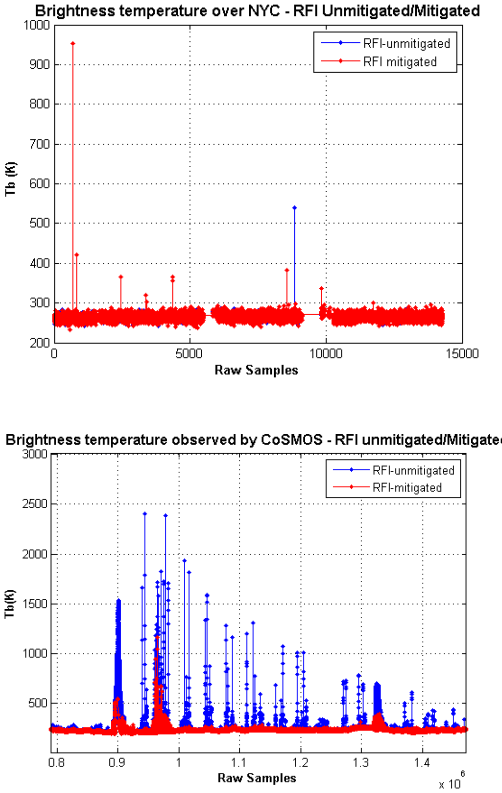

Fig. 1. Brightness temperature values over (a) New-York and (b) Central Europe indicating RFI (blue-unmitigated Tb, red-RFI mitigated Tb using full-band kurtosis)

Studies on the kurtosis statistic have found the algorithm to be extremely sensitive to low duty-cycle pulsed RFI and slightly less sensitive to continuous-wave (CW) type RFI [3,4]. For a pulsed-sinusoid type RFI, the kurtosis

detection algorithm has a blind-spot for a 50% duty-cycle signal. Alternate higher-order algorithms like [5] have been proposed to supplement the kurtosis algorithm.

Most field campaigns at L-band have shown RFI to be of a pulsed nature, and kurtosis has high detectability for such RFI sources. In spite of the success of the kurtosis algorithm, there have been certain isolated cases where the detection algorithm has been unable to detect obvious high power RFI corrupted samples as shown in Fig. 1. The plots indicate two separate field campaign results, SMAPVEX in the Fall of 2008 over New York, and CoSMOS in 2008 over central Europe. As shown, most of the RFI corrupted samples are detected, yet a few high-power samples remain undetected which can wash-out and cause low-level errors if consecutive integration periods are averaged together. One explanation is that these RFI sources have a 50% duty-cycle compared to the radiometric integration period. This is unlikely, since the statistics do not behave similar to a 50% duty-cycle signal when tested under combined integration periods [14].

III. MULTIPLE SOURCE RFI MODEL

In previous literature [2-5, 10], RFI has been modeled as a single pulsed-sinusoidal source. This assumption was valid for L-band since most RFI expected is from air-defense and air-traffic control radars [11]. Though the 21 cm hydrogen line is protected, recent experience from field campaigns (Fig. 1) and results observed from SMOS indicate certain RFI elements exist in-band that might not be radar sites. Also, at other frequencies such as C-, X-, and K-band low-powered multiple RFI sources might exist within the antenna footprint which needs to be taken into consideration for evaluation of the kurtosis detection algorithm.

The improved RFI model assumes multiple pulse sinusoidal sources, and is shown below,

$$x(t) = n(t) + \sum_{i=1}^{N} A_i \cos(\omega_i t + \phi_i) rect\left(\frac{t - t_0}{w_i}\right) \qquad t \in [0, T] \tag{1}$$

where, $n(t) \sim N(0, \sigma^2)$ is normally distributed with standard deviation σ. A is the amplitude of the RFI source, ω is the circular frequency, ϕ is the phase shift, t_0 represents the center of the on pulse of the duty-cycle, w is the width of the on pulse and T is the integration period. The ratio ($d=w/T$) represents the duty-cycle of the RFI source. ω is assumed to be uniformly distributed between [0, $2\pi B$] where B is the bandwidth of the radiometer. ϕ and t_0 are assumed to be uniformly distributed between [$0, 2\pi$] and [$0, T$] respectively. N is the total number of RFI sources.

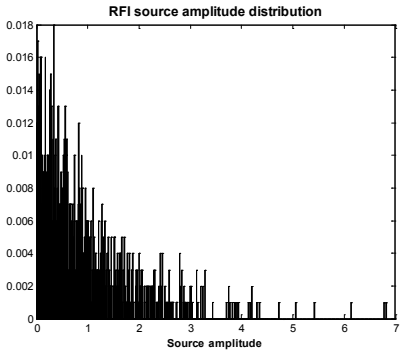

Fig. 2. Exponential distribution applied for amplitude of individual RFI sources, the mean of the exponential distribution is a variable parameter

Within a satellite antenna footprint, the sources are expected to be of various power levels depending on their individual properties and location with respect to the antenna main-lobe and side-lobes. As a result, A is assumed to have an exponential distribution with most of the RFI sources being low-power and a few RFI sources having high power represented by the tail of the distribution. This is shown by Fig. 2. For the duty-cycle of the RFI sources, a bimodal distribution is assumed, indicating the most sources are either very low duty-cycle sources or near CW distribution. This is represented by a combination of a Rayleigh distribution for the low duty-cycle end and inverted exponential distribution for the high duty-cycle end. The fraction that is low duty-cycle is a parameter than can be changed. A 50% low-high duty-cycle fraction is shown in Fig. 3.

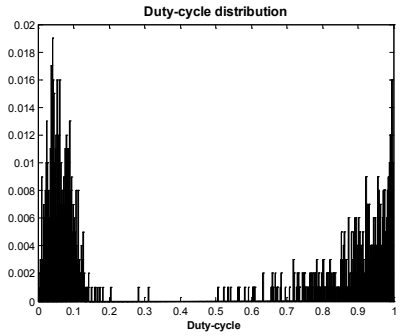

Fig. 3. Bimodal distribution applied for duty-cycle of individual RFI sources, the fraction of low duty-cycle to high duty-cycle is a variable parameter

In order to evaluate the performance of kurtosis in the presence of multiple RFI sources, it is necessary to obtain the probability distribution of the thermal noise with RFI corrupting it. The previous RFI model [3,5] used a probability distribution of a thermal noise source with additive pulse-sinusoidal RFI interference obtained from [12]. Due to multiple sources, the characteristic function of a pulsed-sinusoid source is calculated to obtain the distribution. The characteristic function of the sum of

multiple independent sources is the product of their individual characteristic functions. The probability distribution function of RFI is the Fourier transform of the calculated characteristic function. The probability distribution of (1) is shown below.

$$f(t) = F\left[e^{-\frac{\sigma^2 u^2}{2}} \prod_{i=1}^{N} \left(d_i J_0(A_i u) + (1 - d_i) \right) \right] \quad (2)$$

where J_0 is a zeroth order Bessel function, and $F[\ldots]$ represents the Fourier transform operation.

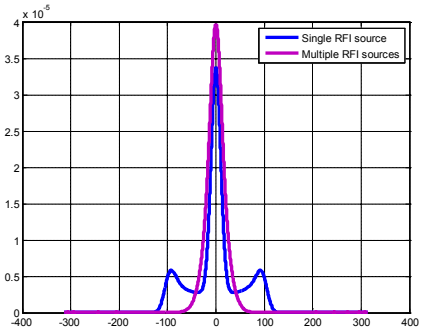

Fig. 4. Probability distribution of RFI with thermal noise (blue-single source, purple-multiple sources)

Fig. 4 shows the probability distribution of a Gaussian signal with a single RFI source, similar to [3,13], and multi-source RFI. These distributions depend on various parameters such as mean power, duty-cycle fraction etc.

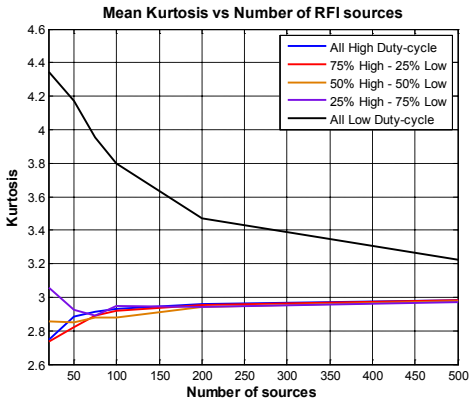

Fig. 5. Mean value of kurtosis vs. increasing number of RFI sources. Different curves represent different fractions of low duty-cycle sources present in the RFI signal

IV. KURTOSIS PERFORMANCE

Based on the assumptions made above, the performance of the kurtosis detection algorithm was assessed considering multiple RFI sources within the antenna footprint. In order to account for the random distribution of duty-cycle and amplitude of the RFI source Monte-Carlo simulations were performed and the average kurtosis ratio and power was considered for each case. Fig. 5 shows the value of the kurtosis ratio with respect to number of sources. There are multiple curves to account for different fractions of low duty-cycle sources within the footprint. As it can be seen from the figure, kurtosis starts getting affected by central-limit theorem for a very high number of sources. The low duty-cycle multiple source RFI is less sensitive to high number of sources and converges slowly towards three. On the other hand, RFI with even a small fraction of CW sources converge towards three faster.

Characterization of RFI in L-band shows that most RFI is in the low duty-cycle [9] and hence would need many sources to be affected by central-limit theorem. Also, more RFI sources results in higher interference power, as shown by Fig. 6. Platforms such as SMAP plan to operate a hybrid of the kurtosis detector and pulse-detector algorithms that can easily identify large RFI jumps. Thus, the issue of central-limit should not be a problem for SMAP because even if kurtosis misses detecting such RFI, large number of sources resulting in high-power RFI should be caught by the pulse-detect algorithm.

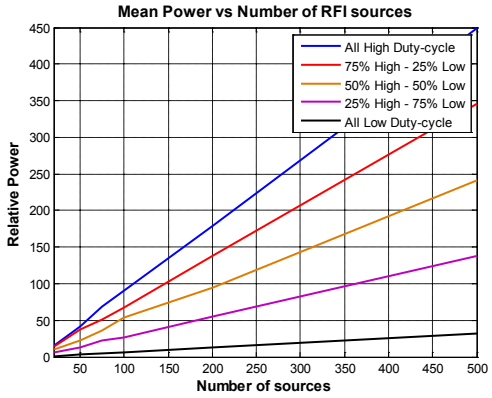

Fig. 6. Mean value of relative RFI power vs. increasing number of RFI sources. Different curves represent different fractions of low duty-cycle sources present in the RFI signal

With the advent of low-power RFID and Wi-Fi systems operating on individual electronic devices in a few years RFI corruption from such devices might not be in the form of an obvious spike (or jump), and might be low enough to be near the NEΔT of the radiometer. The kurtosis detector is capable of detecting spread-spectrum low-power systems [10] but with multiple sources and low power, detection becomes an issue as shown by Fig. 7. The following figure shows the effect on kurtosis observing 200 sources, as the relative power decreases. The rectangular box indicates a region where RFI power is between 0.2 and three times the NEΔT and kurtosis is within three times the NEΔK, the detection threshold of kurtosis assuming ~100K independent samples in an integration period. RFI within this box will be undetectable, yet have a high enough power (above 0.2 NEΔT [20]) to be problematic and impact science measurements.

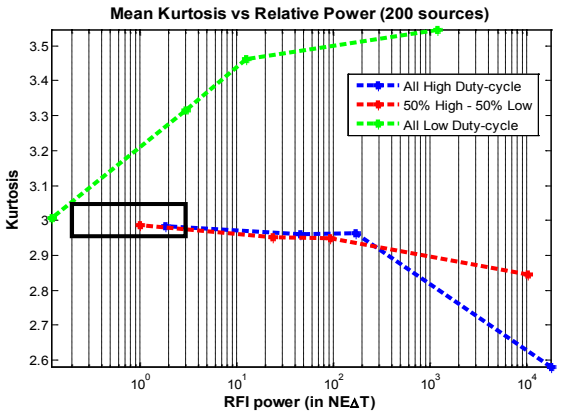

Fig. 7. Mean value of kurtosis vs. RFI power (in NEDT) for 200 sources. (Blue – All high *d*, Red – 50% *d*, Green – All low *d*, Black rectangle – Undetectable problematic RFI)

V. CONCLUSION

The performance of the kurtosis detection algorithm was evaluated for conditions under which multiple RFI sources are present. A new RFI model was developed to replace the single pulsed-sinusoidal RFI model currently used for analysis of RFI detection algorithms. The new RFI model assumes an exponential distribution of RFI power and a bimodal distribution of the duty-cycles of individual RFI sources. Results indicate that the kurtosis algorithm is influenced by the central-limit theorem when enough sources are present. This might cause the kurtosis detection algorithm to miss certain high-powered RFI. The kurtosis algorithm is less sensitive if most of the RFI sources are low duty-cycle sources. SMAP uses pulse-detect algorithm along with the kurtosis detection algorithm, and can easily detect high powered pulses missed by kurtosis. Multiple low-powered Wi-Fi urban RFI sources around the noise-margin of a radiometer can be most detrimental since they are undetectable by either algorithm.

REFERENCES

[1] C.S.Ruf, S.M. Gross and S.Misra, "RFI detection and mitigation for microwave radiometry with an agile digital detector," *IEEE Trans. Geosci. Remote Sensing,* vol 44, pp 694-706,2006

[2] Misra, S., Mohammed, P.N., Guner, B., Ruf, C.S., Piepmeier, J.R., and Johnson, J.T., "Microwave Radiometer Radio-Frequency Interference Detection Algorithms: A Comparative Study,"*IEEE Trans. Geosci. Remote Sensing,* vol. 47(11), pp 3742-3754, 2009

[3] De Roo, R.D., S. Misra and C.S. Ruf (2008). "Sensitivity of the kurtosis statistic as a detector of pulsed sinusoidal RFI, " *IEEE Trans. Geosci. Remote Sensing,* vol. 45, pp. 1938-1946, 2008.

[4] Guner, B., Niamsuwan, N., and Johnson, J. T., "Performance Study of a Cross-Frequency Detection Algorithm for Pulsed Sinusoidal RFI in Microwave Radiometry ," *IEEE Trans. Geosci. Remote Sensing,* vol 48(7), pp 2899-2908, 2010

[5] R. D. De Roo and S. Misra, "A moment ratio RFI detection algorithm that can detect pulsed sinusoids of any duty cycle," *IEEE Geosc Remote Sensing Let.*, vol. 7(3), pp. 606-610, July 2010.

[6] Ruf, C., S. Misra, S. Gross and R. De Roo, "Detection of RFI by its Amplitude Probability Distribution," *Proc. IEEE Geosc. Remote Sensing Symposium,* Denver, CO, 31 Jul -4 Aug 2006.

[7] Misra, S., and C. S. Ruf, "Detection of Radio Frequency Interference for the Aquarius Radiometer," *IEEE Trans. Geosci. Remote Sensing.*, vol. 46(10), 3123-3128, 2008.

[8] Skou, N., Misra, S., Balling, J.E., Kristensen, S.S. and Sobjaerg, S.S., "L-Band RFI as Experienced During Airborne Campaigns in Preparation for SMOS ," *IEEE Trans. Geosci. Remote Sensing,* vol 48(3), pp 1398-1407

[9] S. Misra and C. S. Ruf, "Characterization of L-band RFI across the continental USA using a kurtosis detector," *Proc. IEEE Geosc. Remote Sensing Symposium*, Cape Town, S.A., 2009.

[10] Misra, S., C. Ruf and R. Kroodsma, "Detectability of Radio Frequency Interference due to Spread Spectrum Communication Signals using The Kurtosis Algorithm," *Proc. IEEE International Geoscience and Remote Sensing Symposium*, Boston, MA, Vol. II, 335-338, 7-11 July 2008.

[11] J. R. Piepmeier and F. A. Pellerano, "Mitigation of terrestrial radar interference in L-band spaceborne microwave radiometers," *Proc. IEEE Geosci. Remote Sensing Symposium,* Denver, CO, 31 Jul -4 Aug 2006., pp. 2292–2296.

[12] S. O. Rice, "Statistical properties of a sine wave plus random noise," *Bell Syst. Tech. J.*, vol. 27, no. 1, pp. 109–157, Jan. 1948.

[13] De Roo, R.D., and S. Misra, "A Demonstration of the Effects of Digitization on the Calculation of Kurtosis for the Detection of RFI in Microwave Radiometry," *IEEE Trans. Geosci. Remote Sensing*., vol. 46(10), 3129-3136, 2008.

[14] Misra, S., and C. Ruf, "Inversion Algorithm for Estimating Radio Frequency Interference Characteristics Based on Kurtosis Measurements," *Proc. IEEE International Geosci. and Remote Sensing Symposium*, Cape Town, S.A., Vol. II, 162-165, 13-17 July 2009.

[15] Le Vine, D.M., "ESTAR Experience with RFI at L- band and Implications for Future Passive Microwave Remote Sensing from Space," *Proc. IEEE Geosci. Remote Sensing Symposium,* Toronto, Canada.

[16] Li, L., et al., "A preliminary survey of radio-frequency interference over the U.S. in Aqua AMSR-E data," *IEEE Trans. Geosci. Remote Sensing.*, vol. 42(2), pp. 380-380.

[17] Njoku E.G., P. Ashcroft, T.K. Chan, L. Li, "Global survey and statistics of radio-frequency interference in AMSR-E land observations" *IEEE Trans. Geosci. Remote Sensing.*, vol. 43(5), p.p. 938–947.

[18] Ellingson, S.W. and J.T. Johnson, "A polarimetric survey of radio frequency interference in C- and X-bands in the continental United States using WindSat radiometry," *IEEE Trans. Geosc. Remote Sensing*., vol. 44, 540-548.

[19] National Research Council, Earth Science and Applications From Space: National Imperatives for the Next Decade and Beyond. Washington, DC: National Academies Press, 2007.

[20] ITU, "Interfernce criteria for satellite passive remote sensing," Recommendation ITU-R RS.1029-2, International Telecommunications Union, Geneva, Switzerland, 2003